

polysaccharide (1.25 mg) in water (0.8 mL). After incubation for 1 h at 37 °C and then storage for 15 h at 5 °C, the antigen-antibody complex was pelleted by centrifugation (10000 rpm).

**Reaction of Type a Capsular Polysaccharide with 7-Amino-4-methylcoumarin/EDAC.** The polysaccharide (strain Fin-35, 50 mg, 0.13 mmol) was dissolved in water (5 mL) and then reacted with 7-amino-4-methylcoumarin (126 mg, 0.7 mmol in 2 mL of water) and EDAC (230 mg, 1.2 mmol in 2 mL of water) for 24 h at 25 °C. After filtration of the undissolved coumarin and processing as described in the preceding section, the UV absorbance of the lyophilized product ( $2.95 \times 10^{-3}$  M repeating unit,  $A_{354} = 0.30$ ) was compared with that of a 7-amino-4-methylcoumarin ( $1.50 \times 10^{-6}$  M) plus type a polysaccharide ( $2.95 \times 10^{-3}$  M repeating unit) standard sample ( $A_{354} = 0.03$ ); 46% yield.  $^1\text{H NMR}$  (100 MHz): (normalized  $\text{CH}_3$  signal intensity)/(normalized carbohydrate signal intensity) = 0.0071; 65% yield.

**Acknowledgment.** G.Z. is grateful to the FDA Bureau of Biologics for financial support as an Intergovernmental Personnel

Act assignee to the Division of Bacterial Products and for an appointment as Visiting Scientist in the Division of Biochemistry and Biophysics. We thank Dr. Fai-Po Tsui for preparations of type f capsular polysaccharide, Dr. Frank A. Robey for carrying out ESR measurements, and Dr. Arthur B. Karpas for assistance in chromatographic separations. Stimulating discussions with Dr. John B. Robbins are also gratefully acknowledged.

**Registry No.** EDAC, 25952-53-8;  $\text{CH}_3\text{ONH}_2\cdot\text{HCl}$ , 593-56-6; GalNAc  $\text{C}_3$  monophosphate, 81158-42-1; 3-(OAc)GalNAc  $\text{C}_1$  monophosphate, 81158-43-2; GlcNAc  $\text{C}_4$  monophosphate, 81158-44-3; 4-(OPD $_2$ H $_2$ )GlcNAcO acetylated, 81158-45-4; AAD, 1071-93-8; Tempo-NH $_2$ , 14691-88-4; D-ribosyl 2,3-cyclophosphate, 81158-46-5; D-ribitol 4,5-cyclophosphate, 81203-22-7; D-ribosyl 3-phosphate, 81158-47-6; D-ribitol 5-phosphate, 35320-17-3; D-ribose, 50-69-1; (E)-D-ribosyl O-methyl oxime, 81203-23-8; (Z)-D-ribosyl O-methyl oxime, 81203-24-9; galactosyl  $\text{C}_3$ ,  $\text{C}_4$ -cyclophosphate, 81158-48-7; 7-amino-4-methylcoumarin, 26093-31-2.

## Proton-Nuclear Spin Relaxation and Molecular Dynamics in the Lysozyme-Water System

William M. Shirley and Robert G. Bryant\*

Contribution from the Department of Chemistry, University of Minnesota, Minneapolis, Minnesota 55455. Received July 1, 1981

**Abstract:**  $^1\text{H NMR}$  relaxation measurements are reported for lyophilized lysozyme rehydrated through the gas phase to 0, 13, and 21 g of water/100 g of protein. Protein proton and water proton magnetizations were monitored simultaneously, and the applicability of the cross-relaxation model describing exchange of magnetization between these two spin baths at high temperatures is supported in detail. At the lowest temperatures, water motion becomes sufficiently slow that the separation between water and protein baths is no longer observed; in this region the water protons simply add to the relaxation load of the solid which is dominated by the rotating methyl groups. Analysis of the relaxation parameters derived from the cross-relaxation analysis requires inclusion of the effects of anisotropic water molecule motion in order that the activation parameters for water reorientation are reasonable when compared with thermodynamic measures of the water-protein interaction.

### Introduction

Water is a crucial component of living systems. Understanding water in the complex soup of cytosol is complicated by its interaction with many structures of diverse composition ranging from small solute ions to macroscopic surfaces. The present study is part of an attempt to understand better the dynamical properties of water in the water-protein interface. To simplify the physical problem, we have chosen to immobilize the protein, i.e., to eliminate bulk rotational motion of the protein molecules by studying lyophilized powders rehydrated through the gas phase to various water contents. The possibility that the relatively dry state of the proteins studied here offers a nonnative and possibly inactive conformation is not of great concern because we are confident that the major features of the water-protein interaction are preserved despite minor protein conformation changes.

Nuclear magnetic resonance relaxation is among the useful and direct methods of studying the dynamics of the water-protein interaction.<sup>1-3</sup> Many NMR studies of the water on surface systems have been incomplete because proper account of magnetic interactions between water protons and protein protons has not been included. Though several have taken this magnetic cross-relaxation into account,<sup>4-9</sup> to date there has not been a data set sufficiently complete to test all aspects of the relaxation models

over wide temperature ranges. We have, therefore, measured  $^1\text{H NMR}$  relaxation for protein protons and water protons simultaneously over a wide temperature range for lysozyme powder systems at several water contents and isotopic compositions. The results provide a basis for a critical evaluation of the several models used to interpret such data.

In particular we monitor the protein proton and water proton magnetization simultaneously and check their initial amplitudes and time dependence against the predictions of the cross-relaxation model most clearly formulated by Edzes and Samulski.<sup>7</sup> From careful analysis of the response to selective excitation, we extract the cross-relaxation-model parameters characterizing the two spin systems, water and protein, and the transfer of magnetization between them. Analysis of the data using approximate strategies is evaluated, and the water relaxation parameters are further analyzed critically in order to draw conclusions about the nature of water-molecule motion at the protein surface. This analysis

(4) Hilton, B. D.; Hsl, E.; Bryant, R. G. *J. Am. Chem. Soc.* **1977**, *99*, 8483-8490.

(5) Bryant, R. G.; Shirley, W. M. "Water in Polymers"; Rowland, S. P., Ed.; American Chemical Society, Washington, D.C., 1980; *ACS Symp. Ser.* **127**, 147-156.

(6) Kruger, G. J., presented at Fourth International Symposium on Magnetic Resonance, Rehovot, Israel, 1971.

(7) Edzes, H. T.; Samulski, E. T. *J. Magn. Reson.* **1978**, *31*, 207-229.

(8) Koenig, S. H.; Bryant, R. G.; Hallenga, K.; Jacob, G. S. *Biochemistry* **1978**, *17*, 4348-4358.

(9) Fung, B. M.; McGaughy, T. W. *J. Magn. Reson.* **1980**, *39*, 413-420.

(1) Pfeifer, H. In "NMR, Basic Principles and Progress"; Diehl, P., Fluck, E., Kosfeld, R., Eds.; Springer-Verlag: New York, 1972; Vol. 7, pp 53-153.

(2) Cooke, R.; Kuntz, I. D. *Ann. Rev. Biophys. Bioeng.* **1974**, *3*, 95-126.

(3) Bryant, R. G. *Annu. Rev. Phys. Chem.* **1978**, *29*, 167-188.

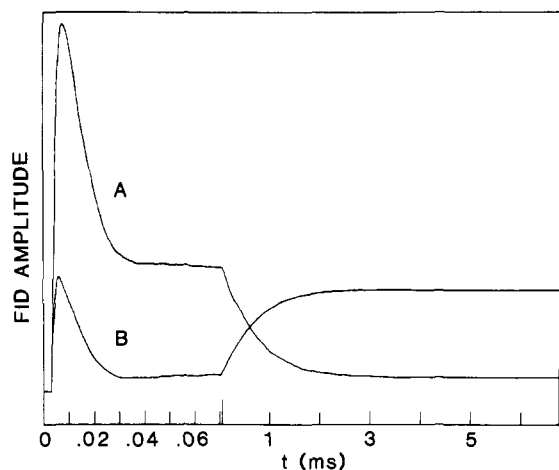


**Figure 1.**  $^1\text{H}$  NMR free induction decays from hydrated lysozyme sample 1H obtained at 57.5 MHz and 284 K for a  $180^\circ\text{-}\tau\text{-}90^\circ$  pulse sequence with a  $91\text{-}\mu\text{s}$   $180^\circ$  pulse and a  $\tau$  of 1.2 s for A and 0.5 ms for B. The  $90^\circ$  pulse ends at  $t = 0$ , and the vertical origin is shifted for B relative to A.

leads to a view of water molecule motion at the surface that includes anisotropic reorientation of water as well as a distribution of activation barriers for reorientation. This view accounts for the known relaxation data without requiring unusual or energetically unreasonable assumptions.

### Experimental Section

**Sample Preparation.** Samples were prepared with hen-egg-white lysozyme (Grade I, Sigma Chemical Co.) that was dialyzed against a solution of 0.01 M EDTA and 0.01 M 1,10-phenanthroline at pH 6 and then dialyzed against deionized water before a final lyophilization. Hydration was accomplished by placing the resulting lysozyme powder in a closed container for about 3 days with the water activity controlled by an appropriate lithium chloride solution. The lysozyme that was hydrated with deuterium oxide was dissolved in deuterium oxide, allowed to stand for 1–12 h, and lyophilized 3 times in order to remove exchangeable protons from the protein. Deuterium oxide (Aldrich, Gold Label, 99.8% D) was passed through a column containing Chelex-100 before equilibration with the lysozyme. The dry sample was prepared by leaving the lysozyme powder in a drying pistol for 48 h at 350 K at pressures less than 0.2 torr. All samples were roughly 50 mg and were sealed in 5-mm NMR tubes and stored below 273 K.

Water contents were determined by Karl Fischer titration or gravimetrically by drying under vacuum at 350 K to constant weight. Sample 2H reported here was one of six duplicate samples. Four of these were analyzed with Karl Fischer titrations, and two, including the one on which NMR measurements were made, were analyzed gravimetrically. The six determinations fell between 12.6 and 14.0 g of water/100 g of lysozyme. The water contents of samples 1H and 2H were found gravimetrically to be  $20.6 \pm 0.6$  g of water/100 g of lysozyme and  $13.3 \pm 0.5$  g of water/100 g of lysozyme, respectively. Karl Fischer titrations were used to find that the samples 1D and 2D contained  $31 \pm 1$  g of  $\text{D}_2\text{O}/100$  g of lysozyme.

**NMR Measurements.** The NMR relaxation measurements were carried out at 57.5 MHz with a pulsed NMR spectrometer that included a 12-inch Varian electromagnetic and a Nicolet NMR-80 data system interfaced with a Biomation 805 waveform recorder. The home-built receiver with probe Q about 50 employed an Optimax AHD-599 preamplifier, which recovers rapidly; however, receiver recovery was limited to about 7  $\mu\text{s}$  primarily because of matching problems between the 1-kW Henry Radio Temp 2006 amplifier and the probe. Nitrogen gas boiled from a liquid nitrogen Dewar and heated by a Varian V-6040 temperature controller was used to adjust the sample temperature measured to  $\pm 2$  K with either a Fluke 2190A digital thermometer or a calibrated diode thermometer.

Spin-lattice relaxation-time measurements were made on resonance with either a  $90^\circ\text{-}\tau\text{-}90^\circ$  or a  $180^\circ\text{-}\tau\text{-}90^\circ$  pulse sequence. The height of the free induction decay (FID) from the protons on the solid was measured 8  $\mu\text{s}$  after the end of the 2–3- $\mu\text{s}$   $90^\circ$  pulse. The  $180^\circ$  pulse was attenuated to an effective pulse length of 90–105  $\mu\text{s}$  as determined by inversion of the water proton magnetization. Some 20–30 repetitions were averaged at each  $\tau$  value, and the dual time base feature of the Biomation 805 was used to record both the rapid and slow decay si-

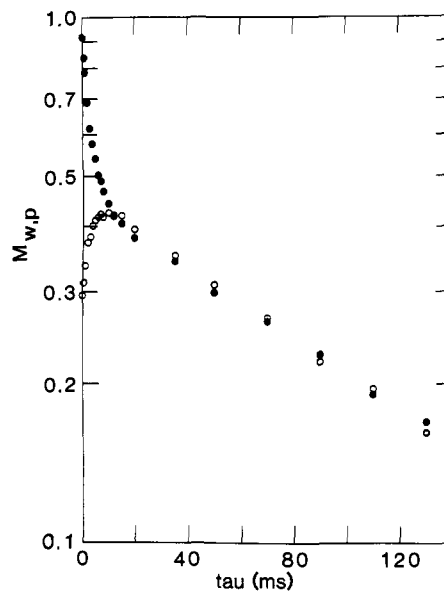


**Figure 2.**  $^1\text{H}$  longitudinal NMR relaxation data obtained at 57.5 MHz from  $180^\circ\text{-}\tau\text{-}90^\circ$  experiments on hydrated lysozyme sample 1H at 267 K in which the  $180^\circ$  pulse width is 91  $\mu\text{s}$ : lysozyme proton results (O) and water proton results (●).

multaneously. Although the least-squares analyses of the data to yield  $T_1$  values indicate high precision, we believe that an error of approximately 5% in  $T_1$  is appropriate. No significant difference in the  $T_1$  value was found when the FID amplitude was measured at 8 or 16  $\mu\text{s}$  for several representative temperatures; thus, within experimental error the results do not depend on where in the FID the amplitude is measured. Though this measure is crude, the solid spin system appears to be in thermal equilibrium with itself.

### Results

The analysis that follows requires precise data, and Figure 1 shows representative raw relaxation data for an hydrated lysozyme powder after the second pulse of the two-pulse inversion recovery sequence. A long  $180^\circ$  pulse was used routinely to enhance the double-exponential character of the spin-lattice relaxation. For FID A the magnetization had completely relaxed before application of the  $90^\circ$  pulse, and maximum FID amplitudes were obtained for both the lysozyme protons and the water protons. The delay time of 500  $\mu\text{s}$  used for FID B is sufficiently short to cause substantial inversion of the water signal and to decrease the amplitude of the solid proton signal. Since the 91- $\mu\text{s}$   $180^\circ$  pulse is not short with respect to the transverse relaxation time of the solid lysozyme protons, the solid magnetization does not invert for any delay time.

Representative relaxation data resulting from the  $180^\circ\text{-}\tau\text{-}90^\circ$  sequence are plotted in Figure 2 as  $M_{w,p} = (S_\infty - S)/2S_\infty$  vs. the delay time,  $\tau$ .  $S$  represents the amplitude of the water or protein FID while  $S_\infty$  refers to this amplitude after a pulse separation that is very long compared with the associated longitudinal relaxation times. It should be noted that  $M_\infty$  at  $\tau = 0$  never quite reaches 1.0 since, even for the water protons, the unattenuated  $90^\circ$  pulse approximate an infinitely short pulse much better than does the attenuated  $180^\circ$  pulse. The relaxation curves for all the  $180^\circ\text{-}\tau\text{-}90^\circ$  experiments were fitted to the equation

$$M_{w,p} = C_{w,p}^+ \exp(-R_f \tau) + C_{w,p}^- \exp(-R_s \tau) \quad (1)$$

with a nonlinear least-squares program, and the results are presented in Table I. The fast and slow relaxation rates,  $R_f$  and  $R_s$ , found from this analysis of the signal from the water protons are generally within experimental error of the  $R_f$  and  $R_s$  values found from analysis of the protein proton signal. The good agreement between these two different measurements is a critical indicator of the experimental precision. The  $C_w^-$  and  $C_p^-$  for the same temperature are also approximately equal; thus the slow component of the  $M_w$  and the  $M_p$  curves are essentially coincident.

Table I. Parameters Obtained by Fitting the Relaxation Data to the Equation  $M_{w,p}(t) = C_{w,p}^+ e^{-R_f t} + C_{w,p}^- e^{-R_s t}$ 

<i>T</i> , K	$C_w^+$	$C_w^-$	$C_p^+$	$C_p^-$	water		protein	
					$10^{-2}R_f$	$R_s$	$10^{-2}R_f$	$R_s$
Sample 1H (20.6 ± 0.6 g of H <sub>2</sub> O/100 g of Lysozyme)								
293	46.9 (5)	47.1 (4)	-19.2 (3)	49.5 (3)	1.86 (4)	6.85 (10)	1.83 (7)	6.34 (6)
283	48.2 (6)	45.4 (5)	-18.9 (3)	48.5 (3)	2.03 (6)	7.01 (15)	2.15 (9)	7.09 (7)
276	47.0 (6)	44.4 (5)	-19.6 (4)	46.0 (4)	2.40 (7)	7.64 (15)	2.42 (13)	7.12 (11)
267	46.6 (6)	44.9 (4)	-17.7 (4)	46.8 (3)	3.05 (10)	7.58 (15)	3.13 (16)	8.13 (9)
258	45.3 (4)	42.7 (3)	-17.8 (2)	44.3 (1)	3.60 (8)	7.80 (11)	3.85 (11)	8.16 (5)
251	43.8 (6)	44.0 (3)	-15.0 (4)	44.2 (2)	5.01 (18)	7.89 (15)	5.29 (33)	7.47 (8)
243	37.5 (5)	41.1 (2)	-13.1 (3)	42.1 (1)	5.54 (17)	7.27 (11)	5.95 (33)	7.31 (6)
234	32.1 (6)	40.8 (2)	-9.9 (5)	41.1 (2)	8.02 (32)	6.61 (10)	7.70 (87)	6.79 (9)
226	31.3 (7)	38.7 (3)	-7.3 (3)	38.8 (1)	11.2 (5)	6.06 (12)	11.5 (10)	5.50 (5)
219	31.7 (6)	37.0 (3)	-6.0 (3)	36.7 (1)	15.4 (7)	5.13 (12)	16.0 (18)	5.15 (6)
211	28.7 (17)	34.9 (6)	-4.8 (5)	33.3 (2)	21.2 (27)	4.90 (29)	16.7 (41)	4.67 (10)
Sample 2H (13.3 ± 0.5 g of H <sub>2</sub> O/100 g of Lysozyme)								
323	50.0 (7)	44.0 (5)	-14.5 (3)	44.9 (2)	3.57 (5)	5.28 (6)	3.46 (19)	5.08 (6)
318	49.8 (12)	42.6 (8)	-12.3 (12)	42.3 (6)	3.35 (20)	5.38 (25)	4.12 (92)	5.28 (22)
313	48.4 (6)	43.6 (4)	-13.0 (3)	44.1 (2)	3.29 (9)	5.48 (11)	3.60 (19)	5.25 (5)
303	49.1 (4)	42.5 (3)	-13.2 (3)	42.5 (2)	3.71 (8)	5.44 (8)	3.99 (20)	5.37 (5)
294	50.0 (5)	41.7 (4)	-12.2 (5)	41.9 (3)	4.54 (16)	5.67 (15)	4.16 (38)	5.49 (9)
286	46.4 (8)	41.0 (4)	-11.8 (5)	41.0 (3)	4.91 (19)	5.77 (15)	4.17 (40)	5.46 (6)
277	45.4 (7)	39.7 (3)	-10.7 (3)	39.5 (1)	6.17 (24)	5.57 (13)	6.32 (37)	5.42 (4)
274	42.8 (6)	40.3 (3)	-10.7 (3)	39.6 (1)	6.34 (20)	5.44 (11)	7.52 (42)	5.15 (5)
270	42.2 (6)	39.9 (3)	-10.1 (2)	39.2 (1)	7.08 (24)	5.22 (12)	8.10 (50)	5.11 (5)
263	41.2 (10)	37.2 (5)	-9.2 (3)	37.3 (1)	8.05 (46)	5.38 (19)	9.55 (60)	5.12 (4)
257	39.0 (7)	37.0 (4)	-8.1 (2)	37.5 (1)	9.63 (44)	5.09 (16)	12.1 (6)	4.82 (3)
250	39.4 (8)	35.8 (4)	-6.1 (3)	35.9 (2)	13.1 (7)	4.64 (16)	11.5 (16)	4.62 (7)
243	26.4 (10)	37.1 (5)	-3.8 (2)	38.8 (1)	10.8 (10)	3.98 (18)	14.5 (17)	4.33 (3)

<sup>a</sup> The estimated standard deviations for the least significant figures are given in parentheses.

Longitudinal proton NMR relaxation rates are shown in Figure 3 for lysozyme at 13.3 and 20.6 g of water/100 g of lysozyme. Data are presented for measurements obtained using both 90- $\tau$ -90° and 180- $\tau$ -90° pulse sequences on both the water proton and the protein proton signals. The presence of water on the lysozyme is seen to lower drastically the spin-lattice relaxation time relative to the dry system and to produce a definite minimum in the vicinity of 273 K. As the temperature is lowered and the water FID gradually becomes unresolvable from the protein proton signal, the  $T_1$  of the hydrated lysozyme increases until it becomes equal to that of the dry lysozyme near the minimum in the dry-lysozyme relaxation curve. At still lower temperatures, the relaxation time in the hydrated sample is somewhat longer than in the dry sample. The only points that may have an error of more than 5% are in the region where the  $T_2^*$  for the water protons approaches that of the solid proton signal. Several 90- $\tau$ -90° measurements were made in the same temperature range as the 180- $\tau$ -90° measurements, and the relaxation times found with the two different pulse sequences agree within experimental error.

In the cross-relaxation analysis that follows, an important parameter is  $F$ , the ratio of the number of protein protons to the number of water protons in the two spin baths. If the cross-relaxation analysis is strictly accurate, the value of  $F$  determined from the FID components should match the analytical values determined by chemical or gravimetric analysis of the water content of the sample. One apparently confusing aspect of the measurements is the inconsistency between the water contents, and thus the  $F$  parameters, as determined analytically and by analysis of the FID amplitudes. So that the water contents from the FID amplitudes could be found, about 35 points on the FID following the 90° pulse after a  $\tau_{\infty}$  delay were fitted to the function

$$M = a \exp(-bt^2) + c \exp(-dt)$$

with a nonlinear least-squares program. Several representative FID curves were decomposed into contributions from the water and the protein protons. Within experimental error straight lines were obtained on semilog paper when the protein FID was plotted vs.  $t^2$  and the water FID plotted vs.  $t$ . Thus, the assumption that the protein resonance has a Gaussian shape and the water resonance a Lorentzian shape appears valid as expected, so that the amplitude ratio,  $a/c$ , should equal  $F$ , the ratio of protein protons to water

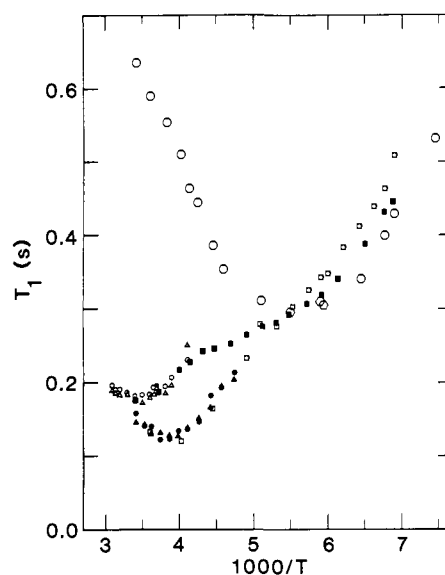
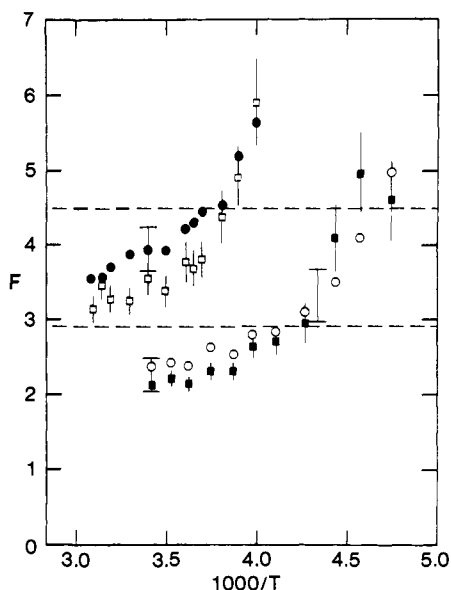


Figure 3. <sup>1</sup>H longitudinal NMR relaxation times for dry lysozyme (○), sample 1H (□), and sample 2H (■) obtained by using the 90- $\tau$ -90° pulse sequence. The remaining points are the  $R_s^{-1}$  values obtained from Table I: sample 1H lysozyme protons (●) and water protons (▲); sample 2H lysozyme protons (○) and water protons (△).

protons. The uncertainty in this method of deriving  $F$  was checked at 293 K for samples 1H and 2H and at 230 K for sample 1H by making from five to ten measurements of  $F$  on different days with slightly misadjusted pulse lengths or detector phases. The ranges of these  $F$  values are indicated in Figure 4 and are much larger than the uncertainties indicated by the least-squares program. With this rather large potential for instrumental uncertainty, we cannot rule out the possibility that systematic errors consistently yield NMR derived  $F$  values lower than the values obtained from gravimetric analysis. However, the presence of a gradual increase in the protein FID amplitude at the expense of the water FID amplitude as the temperature is lowered, which is apparent when Boltzmann factor corrections are included, seems undeniable.



**Figure 4.**  $F$  values found for hydrated samples of lysozyme obtained by different methods. The dashed lines indicate the values calculated for samples 1H and 2H from gravimetric analysis at room temperature using a lysozyme molecular weight at 14 300. Circles indicate the  $F$  values obtained from the ratios of the free induction decay amplitudes for sample 1H (○) and 2H (●) with uncertainties indicated at 293 K for both samples and at 230 K for sample 1H only. The squares indicate  $F$  values obtained for sample 1H (■) and 2H (□) by using a five-parameter least-squares fit to the cross-relaxation-model equations as indicated in the text. The error bars indicate the standard deviations from the least-squares fit.

The spin-lattice relaxation times for the protein protons of the lysozyme samples hydrated with deuterium oxide are shown with the dry-lysozyme data for comparison in Figure 5. These data reflect the contamination of the samples with mobile protons. By finding  $F$  for these samples from the FID ratios as described for sample 1H and 2H, the deuterium oxide on the lysozyme was estimated to contain 26% and 11% H for samples 1D and 2D, respectively, while the nominal water content was 31 g of  $D_2O/100$  g of lysozyme. The relaxation times near room temperature are lower for sample 1D than for 2D, and both samples have  $^1H$   $T_1$  values lower than the dry sample. As the temperature is lowered, the relaxation times for the two lysozyme- $D_2O$  samples increase until they equal the  $T_1$  of the dry lysozyme. The relaxation times of all three samples remain equal down to 200 K, but at the  $T_1$  minimum and lower temperatures, the  $T_1$  values for samples 1D and 2D remain somewhat below the values for the dry lysozyme. In a previous investigation,<sup>5</sup> a power sample with 7 g of  $D_2O/100$  g of lysozyme gave  $T_1$  values between 273 and 180 K almost coincident with the dry-lysozyme curve in Figure 5.

## Discussion

**Magnetic Cross Relaxation.** Nonexponential NMR relaxation may arise from several sources, including slow diffusion of molecules to relaxation sinks, slow chemical-exchange mixing of two or more spin populations, and magnetic exchange or cross relaxation between two spins or spin populations. The present understanding of the markedly nonexponential NMR relaxation in the water-solid protein systems involves the dominance of cross-relaxation effects, which were first pointed out by Kruger<sup>6</sup> for protein powders and discussed by several groups since.<sup>4,7-9</sup> The effects of cross relaxation are pervasive. In protein solutions the protein protons increase the water proton relaxation rate, while in the solid case, the water protons provide a relaxation path for the protein protons. The present experiments provide sufficient data to test this model carefully and examine its limitations.

The cross relaxation model as discussed by Koenig and co-workers treats the protein protons and the water protons as two separate thermodynamic systems that interact magnetically.<sup>7,8</sup>

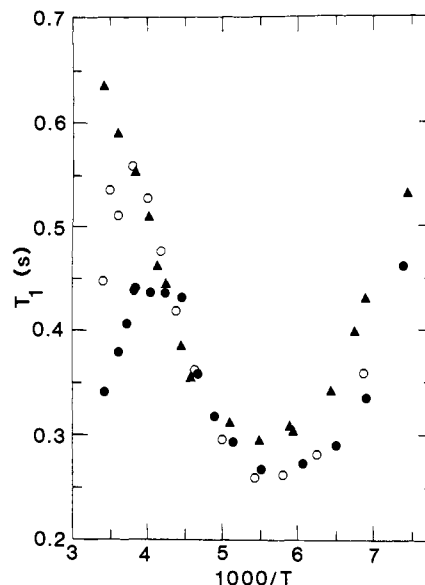


**Figure 5.** Lysozyme proton longitudinal relaxation times obtained at 57.5 MHz shown as a function of reciprocal temperature for dry lysozyme (▲); lysozyme rehydrated with deuterium oxide, samples 1D (●) and 2D (○).

This model leads to the coupled equations

$$\begin{aligned} dM_w/dt &= -(R_w + R_t)M_w + R_tM_p \\ dM_p/dt &= -(R_p + R_t/F)M_p + R_tM_w/F \end{aligned} \quad (2)$$

The  $R_p$  and  $R_w$  are the protein and water proton spin-lattice relaxation rates, and  $R_t$  is the rate of magnetization transfer between the two spin systems.  $M_w$  and  $M_p$  are normalized magnetizations defined earlier, and  $F$  is the ratio of protein protons to water protons. Solutions of eq 2 are given by eq 1 in which the experimentally obtained parameters are related to those of the model in eq 3, where eq 3a requires the use of a plus sign with  $R_{f,s} = \{(R_w + R_p + R_t + R_t/F) \pm [(R_p - R_w - R_t + R_t/F)^2 + 4R_t^2/F]^{1/2}\}/2$  (3a)

$$C_w^\pm = \pm[(R_w - R_{s,f})/(R_f - R_s)]M_w(0) \pm [R_t/(R_f - R_s)][M_w(0) - M_p(0)] \quad (3b)$$

$$C_p^\pm = \pm[(R_p - R_{s,f})/(R_f - R_s)]M_p(0) \mp [(1/F)(R_t/(R_f - R_s))][M_w(0) - M_p(0)] \quad (3c)$$

$R_f$  and a minus sign with  $R_s$ . If both pulses in a  $180-\tau-90^\circ$  sequence are much shorter than the transverse relaxation times for both the water and the protein protons, the normalized magnetizations immediately after the first pulse,  $M_w(0)$  and  $M_p(0)$ , are equal, and the relaxation equations simplify to give

$$R_{w,p} \approx C_{w,p}^+R_f + C_{w,p}^-R_s \quad (4)$$

However, with short pulses the double-exponential character of the relaxation is not distinct, making extraction of the model parameters difficult. A soft first pulse in the  $180-\tau-90^\circ$  experiment makes the double-exponential decay obvious by making  $M_w(0)$  greater than  $M_p(0)$ , but it invalidates the approximation represented in eq 4. However, the approximations

$$\begin{aligned} R_w &\approx [R_s - (1 - p_w)R_p]/p_w \\ R_t &\approx R_fF/(1 + F) \end{aligned} \quad (5)$$

where  $p_w$  is the fraction of water protons in the sample, are valid for short or long pulses under the usual conditions  $R_t, R_t/F \gg R_w, R_p$ .

The hydrated lysozyme data shown in Figures 2 and 3 demonstrate clearly that a cross relaxation dominates spin relaxation

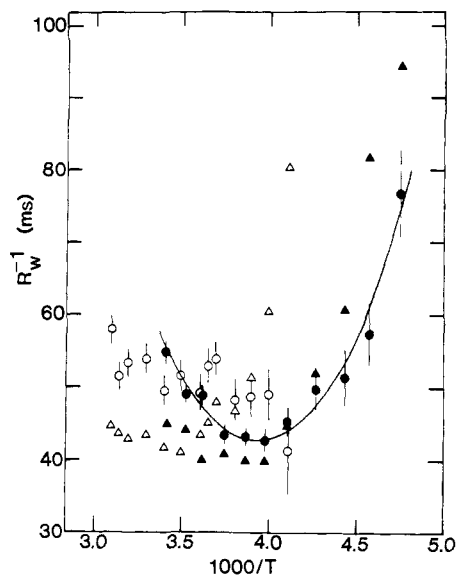


**Figure 6.** Temperature dependence of the reciprocal relaxation rate  $R_w^{-1}$  for samples 1H (closed symbols) and 2H (open symbols) calculated with the following procedures: triangles obtained with approximation 5 with  $p_w$  from the dehydration results and  $R_p$  from the dry-lysozyme values; circles from a five-parameter least-squares procedure, with  $R_w$ ,  $R_t$ ,  $M_w(0)$ ,  $M_p(0)$ , and  $F$  allowed to vary and  $R_p$  set to the dry-lysozyme values. Standard deviations from the least-squares program are indicated by the error bars. The solid curve is drawn for sample 1H and represents a least-squares fit to the isotropic form of eq 6, with  $\sigma_0^2 = 8.9 \times 10^9 \text{ s}^{-2}$ ,  $\tau_0 = 3.9 \times 10^{-12} \text{ s}^{-1}$ , and  $\Delta H = 3.1 \text{ kcal/mol}$ .

in these systems. The decay of longitudinal magnetization is nonexponential whether the water protons or the protein protons are observed, and the relaxation rates obtained are essentially identical. The coefficients  $C_p^\pm$  and  $C_w^\pm$  depend on pulse width as predicted by the basic model, and  $C_p^-$  and  $C_w^-$  found experimentally are almost equal as predicted by eq 3 when  $R_t$  is large. Although the major features of the model clearly match the experimental data very satisfactorily, it remains to be seen whether the relaxation rates  $R_p$ ,  $R_w$ , and  $R_t$  have fundamental significance.

The model parameters may be extracted in several ways. Since much of the earlier literature reports only  $R_s$ , evaluation of different and approximate methods is useful. Approximation 5 provides the simplest evaluation of  $R_w$  since only the slow component of the water proton relaxation rate, the water content of the sample, and an estimate of the protein proton relaxation rate are needed. If the complete double-exponential relaxation curve for either the protein protons or the water protons is obtained, the estimated values of  $R_p$  and  $F$  may be fixed in a least-squares fit of the parameters  $R_w$ ,  $R_t$ ,  $M_w(0)$ , and  $M_p(0)$  to the relaxation data.<sup>5</sup> Additional parameters may be incorporated when both the complete protein proton and water proton decay curves are available as in the present case, though exceptional precision is required to avoid large standard deviations in the derived parameters when a six-parameter fit is employed. Except for the six-parameter case, the protein relaxation rate,  $R_p$ , is approximated by the relaxation rate of the dry-lysozyme system. Drying the lysozyme may change the protein proton motion and thus the relaxation rate. A sample hydrated with deuterium oxide may provide a better estimate for this rate; however, comparisons are complicated somewhat by contaminating mobile protons. Comparison of the proton longitudinal relaxation times for the dry lysozyme with those of the lysozyme hydrated with deuterium oxide in Figure 5 shows that the relaxation rates for both types of sample are the same between the dry lysozyme  $T_1$  minimum and the temperature at which the  $T_1$  decreases due to mobile protons in the deuterated sample. Thus, the presence of water does not affect the proton NMR relaxation rate significantly between 190 and 260 K so the dry lysozyme relaxation rate may be taken as a good approximation for  $R_p$ . We may conclude that if water addition does increase the rates of internal protein motions

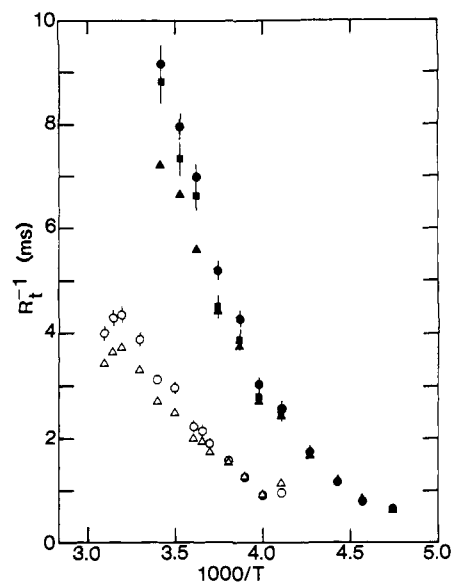


**Figure 7.** The temperature dependence of the reciprocal of the rate of magnetization transfer  $R_t^{-1}$  for sample 1H (closed symbols) and 2H (open symbols) calculated by using the methods indicated in the caption to Figure 6. The squares indicate the results of a six-parameter least-squares procedure.

such as side-chain rotations, these motions remain sufficiently slow that they make at most a very small contribution to protein proton NMR relaxation.

Multiparameter curve fitting may propagate errors in devious ways. Figures 6 and 7 present values of  $R_w^{-1}$  and  $R_t^{-1}$  derived from the raw data in three different ways. The room-temperature values of  $R_w^{-1}$  calculated with approximation 5 are smaller than values found with the five-parameter fit, but at lower temperatures the situation is reversed. In both of these calculations  $R_p$  was taken from an interpolation of the dry-lysozyme protein proton measurements. The differences in these two sets of  $R_w^{-1}$  values are mainly due to the choices made for  $F$ ; the  $F$  value obtained from the dehydration gravimetric measurements was used over the whole temperature range with approximation 5 while  $F$  is permitted to vary in the five-parameter fit and leads to different values at each temperature as summarized in Figure 4. At any particular temperature, a larger  $F$  results in a smaller  $R_w^{-1}$ . Thus, the  $R_w^{-1}$  calculated from the approximate equation at low temperature is longer than the  $R_w^{-1}$  found by the least-squares procedure because  $F$  is fixed in the approximate method while it increases with decreasing temperature in the five-parameter fit. A four-parameter least-squares fit with both  $R_p$  and  $F$  held constant was also made to this data, but the results are not presented because the  $R_w^{-1}$  and  $R_t^{-1}$  values obtained were all within 10% of the approximation 5 results at high temperature with much better agreement at lower temperatures. Compared with the five-parameter fits, the six-parameter fits tend to increase  $R_p$  and decrease  $R_w$  but produce such large standard deviations in these parameters that little is gained by presenting them here. Figure 7 shows that the temperature dependence of  $R_t^{-1}$  is not substantially affected by the refinement procedure. Using approximation 5 to derive  $R_t^{-1}$  gives values that are somewhat low at higher temperatures because the inequality  $R_t \gg R_w$  is less well satisfied. Each least-squares procedure gives  $M_w(0)$  and  $M_p(0)$  values and standard deviations within approximately 1% of those calculated from the FID amplitude coefficients listed in Table I. The  $F$  values derived from the five-parameter fit match well the values obtained from the FID ratio as shown in Figure 4. This agreement arises from two very different aspects of the magnetization behavior and provides strong support for the cross-relaxation model and the data analysis procedures used.

Proton longitudinal relaxation times for dry-lysozyme powders have been reported and interpreted by Andrew, Bryant, and

Cashell.<sup>10</sup> The dominant feature of the data is a  $T_1$  minimum near 180 K, which apparently arises principally from rotating methyl groups. Andrew and co-workers estimate that about 70% of the relaxation comes from the methyl groups while the rest is caused by other motions such as side-chain reorientation. At temperatures below the dry-lysozyme minimum, our hydrated lysozyme results show that the presence of water decreases the protein proton relaxation rate. This observation is understandable if the water molecule motion at these low temperatures is too slow to cause efficient proton relaxation. In this case the water protons add to the solid protein spin system thus increasing the number of spins that must relax through the methyl rotation path. Since the number of methyl groups is constant, the relaxation rate is inversely proportional to the number of protons in the effective solid spin system,<sup>11-13</sup> hence, the observation that water slows the relaxation rate at low temperature. In this temperature range cross relaxation between the water and protein protons obviously occurs, but treatment in terms of separated spin systems each in equilibrium with itself is clearly inappropriate. The water and protein protons relax together, and separation of the spin systems loses significance as expected when  $R_1$  becomes extremely large.

Similar reasoning accounts for the shorter  $T_1$  values observed at low temperatures for the lysozyme-D<sub>2</sub>O samples. By exchange of the protein samples three times before they were hydrated with D<sub>2</sub>O, the average number of protons relaxed by each methyl group is reduced, thus increasing the relaxation rate. Low temperature relaxation data reported by Andrew and co-workers<sup>10,14</sup> showed similar behavior; i.e., there are larger  $T_1$  values for dry lysozyme than for dry lysozyme exchanged with D<sub>2</sub>O, but they attributed the difference to the presence of a small amount of water.

At temperatures above those of the  $T_1$  minimum in dry lysozyme, the spin-lattice relaxation times for the hydrated lysozyme are markedly depressed from those of the dry lysozyme. This result is understandable if water molecule reorientation is sufficiently rapid to provide an efficient relaxation path. Since it is the protein proton  $T_1$  that is measured in this region just above 180 K, cross relaxation of the protein spins by water protons occurs efficiently even at these low temperatures.

**Anisotropic Water Molecule Motion.** Interpretation of  $R_s^{-1}$  or  $R_w^{-1}$  has the greatest potential for illuminating the dynamical details of water molecule motion at the protein surface. The occurrence of a minimum in  $T_1$  implies that the frequency of some motion that modulates the proton dipole-dipole interaction is of the order of the nuclear Larmor frequency. The issue is what motions are possible or likely? Proton exchange is a possible source of time dependence; however, the temperatures and frequencies at which we are working should require hydrogen lifetimes to be long compared to the correlation times sensed by these measurements.<sup>15</sup> We therefore neglect the direct contributions of proton exchange to relaxation. An attractive hypothesis proposed by Woessner to account for NMR relaxation of water adsorbed on surfaces is that at the lowest temperatures studied the onset of water molecule motion involves a simple rotation about a bond that holds the molecule to the surface.<sup>16,17</sup> At higher temperatures or on longer time scales reorientation of this rapid rotation axis would also occur that would correspond to translation of the water molecule on the surface. Stated differently, we may identify the low-temperature motion of adsorbed water molecules with re-

stricted or anisotropic rotation about a hydrogen bond that holds it to a particular site on the protein. Such sites are reported with increasing frequency and precision by X-ray studies,<sup>18</sup> and such a rotational motion is consistent with those reports since the rotation will not change the oxygen atom position. Reorientation of the rotation axis may, though need not, permit movement of water from one site to another on a somewhat longer time scale. However, the absence of observable dipolar or quadrupolar splittings<sup>19</sup> in the lysozyme powder samples requires that motional averaging be complete on the time scale of the order of the splittings involved; i.e., the several motions possible must carry the water molecule through all orientations in a time on the order of 1  $\mu$ s. Separation of rotation and translation of water in crystal systems is known.<sup>20</sup> The concept of localized water motion on the surface is thus similar to methyl relaxation effects. The separation of translational and rotational correlation times implied by the model is one way of looking at the general problem of anisotropic rotational motion at a surface, which was treated generally by Woessner.<sup>21</sup> The relaxation equation becomes where

$$\frac{1}{T_1} = Q \left[ A \left( \frac{\tau_s}{1 + \omega_0^2 \tau_s^2} + \frac{4\tau_s}{1 + 4\omega_0^2 \tau_s^2} \right) + B \left( \frac{\tau_1}{1 + \omega_0^2 \tau_1^2} + \frac{4\tau_1}{1 + 4\omega_0^2 \tau_1^2} \right) + C \left( \frac{\tau_2}{1 + \omega_0^2 \tau_2^2} + \frac{4\tau_2}{1 + 4\omega_0^2 \tau_2^2} \right) \right] \quad (6a)$$

$$\frac{1}{T_2} = \frac{Q}{2} \left[ A \left( 3\tau_s + \frac{5\tau_s}{1 + \omega_0^2 \tau_s^2} + \frac{2\tau_s}{1 + 4\omega_0^2 \tau_s^2} \right) + B \left( 3\tau_1 + \frac{5\tau_1}{1 + \mu_0^2 \tau_1^2} + \frac{2\tau_1}{1 + 4\omega_0^2 \tau_1^2} \right) + C \left( 3\tau_2 + \frac{5\tau_2}{1 + \omega_0^2 \tau_2^2} + \frac{2\tau_2}{1 + 4\omega_0^2 \tau_2^2} \right) \right] \quad (6b)$$

$$Q = \frac{3}{10} \gamma^4 \hbar^2 r^{-6} = 1.438 \times 10^{10} \text{ s}^{-2} \text{ for } r = 1.51 \text{ \AA} \quad (6c)$$

$$A = \frac{1}{4} \langle (3 \cos^2 \Delta - 1)^2 \rangle \quad B = 3 \langle \sin^2 \Delta \cos^2 \Delta \rangle \quad (6d)$$

$$C = \frac{3}{4} \langle \sin^4 \Delta \rangle$$

$$\tau_1^{-1} = \tau_f^{-1} + \tau_s^{-1} \quad \tau_2^{-1} = \tau_s^{-1} + 4\tau_f^{-1} \quad (6e)$$

$\gamma$  is the magnetogyric ratio,  $\Delta$  the angle between the rapid rotation axis and the internorment vector  $r$ ,  $\tau_f$  is the correlation time for the rapid rotation, and  $\tau_s$  is the correlation time for reorientation of the rotation axis; the rotational reorientation is assumed to be diffusional. These equations predict two minima: a low-temperature minimum that reflects slowing of the fast rotation and a higher temperature minimum corresponding to reorientation of the fast-rotation axis. Representative plots of  $T_1$  are shown in Figure 8 as a function of reciprocal temperature for parameter choices that show a clear separation of the dynamical components. It is not clear that both minima of these curves could be resolved in the present study because the high temperature required also drive desorption; however, eq 6 imply that resolution should be possible if measurements are made over a sufficiently wide frequency range.

Inspection of Figure 8 shows that the relaxation equations implied by this model predict several changes in the behavior of the relaxation times compared with the isotropic cases: (1) The depth and position of the low-temperature  $T_1$  minimum is dependent on the choice of the angle  $\Delta$ . (2) Any distribution of the angle  $\Delta$  causes further elevation of the low-temperature  $T_1$

(10) Andrew, E. R.; Bryant, D. J.; Cahsell, E. M. *Chem. Phys. Lett.* **1980**, *69*, 551-554.

(11) Andrew, E. R.; Hinshaw, W. S.; Hutchins, M. G.; Sjöblom, R. O. I. *Mol. Phys.* **1976**, *31*, 1479-1488.

(12) Andrew, E. R.; Hinshaw, W. S.; Hutchins, M. G.; Sjöblom, R. O. I.; Canepa, P. C. *Mol. Phys.* **1976**, *32*, 795-806.

(13) Andrew, E. R.; Hinshaw, W. S.; Hutchins, M. G.; Sjöblom, R. O. I. *Mol. Phys.* **1977**, *34*, 1695-1706.

(14) Andrew, E. R.; Green, T. J.; Hoch, M. J. R. *J. Magn. Reson.* **1978**, *29*, 331-339.

(15) Koenig, S. H.; Schillinger, W. E. *J. Biol. Chem.* **1969**, *244*, 3283-3289.

(16) Woessner, D. E. *J. Chem. Phys.* **1962**, *36*, 1-4.

(17) Woessner, D. E.; Zimmerman, J. R. *J. Phys. Chem.* **1963**, *67*, 1590-1600.

(18) Watenpugh, K. D.; Margulis, T. N.; Sieker, L. C.; Jensen, L. H. *J. Mol. Biol.* **1978**, *122*, 175-190.

(19) Borah, B.; Bryant, R. G. *Bophys. J.* **1982**, *38*, 47-52.

(20) O'Reilly, D. E.; Tsang, T. *J. Chem. Phys.* **1967**, *47*, 4072-4076.

(21) Woessner, D. E. *J. Chem. Phys.* **1962**, *37*, 647-654.

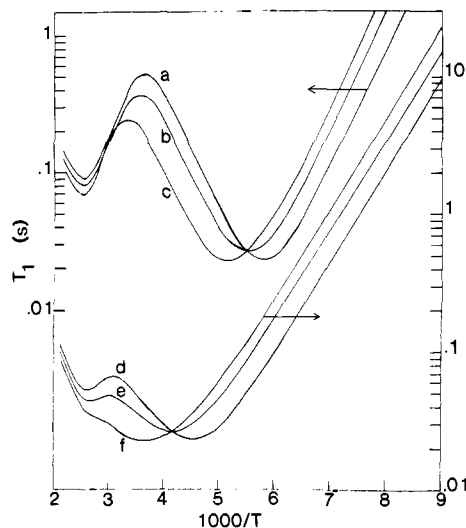


**Figure 8.** Longitudinal relaxation times calculated from the anisotropic model shown as a function of reciprocal temperature. Curves a, b, and c were calculated with arbitrary activation parameters which give a clear separation of minima associated with the two correlation times in the problem. Curves a and d are for  $\Delta = 90^\circ$ , c and f are for  $\Delta = 38^\circ$ , and b and e are for an equal distribution between these two angles. The activation parameters for curves d, e, and f were 3 kcal/mol for the fast process and 7 kcal/mol for the slow process with temperature-independent preexponential parameters of  $7.5 \times 10^{-12}$  and  $2.16 \times 10^{-13}$ , respectively.

minimum. (3) Curves b and e, calculated by assuming an equal distribution of water molecules between angles of 38 and  $90^\circ$ , the angles appropriate to H or O hydrogen-bonded orientations, lead to an elevation of the  $T_1$  minimum of 54% relative to the isotropic case. This effect is less than a factor of 2 and still well below the values of  $R_w^{-1}$ . Therefore, effects of anisotropic motion alone cannot account for the decrease in efficiency of longitudinal relaxation at the minimum. (4) Effects on transverse relaxation are very large. For example, at the minimum in curve e of Figure 8, the corresponding  $T_2$  value is calculated to be 3.2  $\mu\text{s}$ , giving a  $T_1/T_2$  ratio over 5000. Therefore, while the effects on  $T_1$  are small, the consequences of anisotropic motion on the transverse-relaxation rate are great. Thus, interpretations of  $T_1/T_2$  ratios in such systems are difficult in the absence of specific additional information about the motional anisotropy. Though we accept anisotropic water motion at the surface as a very likely possibility, the simple application of it represented in Figure 8 provides an incomplete hypothesis that fails to account for the present data. For simplicity we will temporarily neglect it. The isotropic equations are obtained as a special case of the anisotropic ones by setting  $\Delta$  equal to zero; only the first term survives. A useful property of the equation then is that at the minimum in  $T_1$ ,  $\omega\tau_c = 0.6158$ .

Inspection of eq 5 focusing on the derived values for  $R_w^{-1}$  shows that a minimum in  $R_s^{-1}$  should occur at about the same temperature as a minimum in  $R_w^{-1}$  provided that  $R_s > R_p$  and that  $R_p^{-1}$  is a linear function of reciprocal temperature. These conditions are in agreement with our data. While the five-parameter least-squares  $R_w^{-1}$  curve for sample 1H has a minimum at 255 K, perhaps 5 K lower than that for the  $R_s^{-1}$  curve, the five-parameter least-squares  $R_w^{-1}$  curve for the drier sample (2H) shows no clear minimum. This observation may result simply from poorer data in the lower temperature ranges, and we suspect that the minimum is located at about 290 K as it is for  $R_w^{-1}$ . Thus, with the assumption of isotropic motion, the correlation time reported for the water motion is about  $1.7 \times 10^{-9}$  s near 255 K in sample 1H and has this value at about 290 K in sample 2H.

The transverse-relaxation times were not the focus of this study; however, several observations about the measured  $T_2^*$  values are required. The value of  $T_2^*$ , the time constant for the water FID, is 280  $\mu\text{s}$  at 255 K and approximately the same value for sample 2H at about 290 K. In an earlier study<sup>4</sup> of hydrated lysozyme

at 30 MHz with a somewhat wetter sample (25 g of water/100 g of lysozyme) the value of  $T_2$  is reported to be 400  $\mu\text{s}$  at the poorly resolved  $T_1$  minimum at 230 K. Since the  $T_2$  value at 57.5 MHz should be about half the value at 30 MHz, the  $T_2^*$  values of the present study are consistent with the earlier data. The ratio  $R_w^{-1}/T_2^*$  at the  $R_w^{-1}$  minimum is about 150, significantly smaller than the ratio  $R_s^{-1}/T_2^*$ , but the large ratio clearly implies another major contribution to transverse relaxation. Several possibilities for the depression of  $T_2$  include (1) contributions to  $T_2$  from cross relaxation, (2) contributions from anisotropic motion as calculated in Figure 8, (3) contributions from chemical-exchange modulation of any magnetic interaction, and (4) contributions from a distribution of correlation times. While we anticipate contributions to transverse relaxation from cross relaxation, the usual two-spin treatment is inappropriate the present situation. As indicated earlier, we anticipate that the major contributions of chemical exchange occur at low frequencies; at low temperatures, many of these events should be too slow to dominate even  $T_2$ . The effects of a distribution of correlation times are well known and will be addressed shortly. Inspection of eq 6 clearly shows that the contribution from anisotropic motion may be so overwhelming that the slow motion dominates  $T_2$  and the fast motion dominations  $T_1$ . If we ascribe all of the  $T_1/T_2$  ratio enlargement to the effects of anisotropic motion with an equal distribution between angles of 38 and  $90^\circ$  (an approximation that is inadequate), then  $\tau_s \sim 8.5 \times 10^{-9}$  s at the  $T_1$  minimum.

**Correlation Time Distribution.** A broad minimum in  $T_1$  and a large  $T_1/T_2$  ratio have long been associated with a distribution of correlation times;<sup>22</sup> however, applications of the idea have been made often directly to  $R_s^{-1}$  data for hydrated proteins without regard to the effects of intermolecular cross relaxation. The usual procedure<sup>23</sup> is to assume that a lognormal distribution (eq 7)

$$P(\tau_c) d\tau_c = \beta^{-1} \pi^{-1/2} \exp(-z^2/\beta^2) dz \quad z = \ln(\tau_c/\tau_c^{\text{av}}) \quad (7)$$

describes the distribution of correlation times, with the average correlation time denoted by  $\tau_c^{\text{av}}$ . This distribution is combined with the isotropic version of eq 6, and the data are fitted to the resulting expressions by using least-squares techniques. The four parameters in the analysis are the effective second moment ( $\sigma_0^2 = 0.45 \hbar^2 \gamma^4 r^{-6}$ ), the width parameter ( $\beta$ ), and the usual activation parameters associated with the activation law

$$\tau_c = \tau_0 \exp(\Delta H/RT) \quad (8)$$

The  $R_w^{-1}$  results from the hydrated lysozyme sample 1H were fitted with a modification of a program developed by H. A. Resing in which  $\sigma_0^2$  and  $\beta$  were allowed to vary. The  $\tau_0$  value was determined by the condition that  $\omega\tau_c = 0.6158$  at the minimum while  $\Delta H$  was taken over a range of values spaced by 100 cal. The resulting series of fits were scanned until  $T_2$  values calculated from the model parameters obtained in the  $T_1$  fitting procedure closely matched the experimental  $T_2^*$  values as shown in Figure 9. The parameter resulting from this strategy are  $\Delta H = 11.0$  kcal/mol,  $\tau_0 = 5.84 \times 10^{-19}$  s<sup>-1</sup>,  $\sigma_0^2 = (2.84 \pm 0.05) \times 10^{10}$  s<sup>-2</sup>, and  $\beta = 5.6 \pm 0.2$ . This width parameter would imply that about two-thirds of the water molecules experience correlation times between  $4.6 \times 10^{-7}$  and  $6.3 \times 10^{-12}$  s. The second moment resulting from the fit is somewhat larger than the value of  $2.63 \times 10^{10}$  s<sup>-2</sup> for ice.<sup>24</sup>

The assumption of a correlation-time distribution also implies an apparent phase transition in  $T_2$  that occurs as the correlation times of molecules in the long-correlation-time portion of the distribution become longer than a cutoff time,  $\tau_c^*$ .<sup>22</sup> Such a dependence is indicated in Figure 4 by the increase in  $F$  values for the hydrated lysozyme samples as the temperature is lowered. However, the continuous change in  $F$  may correspond to a real phase change occurring over a temperature range due to the heterogeneity of the hydrated protein. For comparison, Figure 9 shows the fraction of mobile protons  $f_m$  derived from the cutoff

(22) Resing, H. A. *J. Chem. Phys.* **1965**, *43*, 669-678.

(23) Resing, H. A. *Adv. Mol. Relaxation Processes* **1967**, *1*, 109-154.

(24) Kume, K. *J. Phys. Soc. Jpn.* **1960**, *15*, 1493-1501.

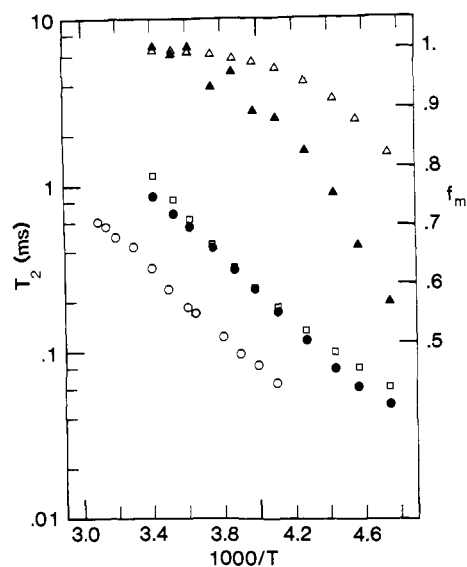


**Figure 9.** Values of  $T_2^*$  for the slowly relaxing part of the free induction decay in samples 1H (●) and 2H (○) at 57.5 MHz. The  $f_m$  (▲) and  $T_2$  values (□) were obtained from the procedure described in the text for application of the distribution of correlation times to the data with  $\Delta H = 11.0$  kcal/mol,  $\tau_0 = 5.84 \times 10^{-19}$  s $^{-1}$ ,  $\sigma_0^2 = 2.84 \times 10^{10}$  s $^{-2}$ , and  $\beta = 5.6$ , and are compared with the data for sample 1H. The  $f_m$  (▲) from sample 1H were calculated from the  $F$  values given in Figure 4 from the relation  $f_m = (1 + F^0)/(1 + F)$ , where  $F^0$  is an average of  $F$  values above 273 K.

assumption. That is,  $1 - f_m$  indicates the molecules whose correlation times have become longer than  $\tau_c^*$ , which is assumed to equal  $\sigma_0^{-1}$ . The  $f_m$  derived in this way remains large to a much lower temperature than is implied by the temperature dependence of  $F$  obtained from the FID ratios shown in Figure 4. A similar difficulty has been reported in a similar analysis of water adsorbed on porous glass.<sup>25</sup>

Though there appears to be little fundamental justification, the results of a similar fitting strategy applied to the  $R_s^{-1}$  data are included for comparison with earlier treatments:  $\Delta H = 11.0$  kcal/mol,  $\tau_0 = 1.05 \times 10^{-18}$  s,  $\sigma_0^2 = (1.10 \pm 0.03) \times 10^{10}$  s $^{-2}$ , and  $\beta = 6.8 \pm 0.3$ . These values provide reasonable agreement with measured  $T_2$  values above 250 K but deviate significantly at lower temperatures. The major problem in this treatment is failure of  $\sigma_0^2$  to agree with reasonable values for other solids like ice; however, this problem is absent when the analysis is made on  $R_w^{-1}$ , i.e., when cross relaxation is taken into account.

The foregoing analysis using the application of the concept of a distribution of correlation times to account for  $T_1$  and  $T_2$  data for water on lysozyme has been applied in the customary fashion and yields results that are not very different from similar applications to other liquids on surfaces.<sup>23</sup> However, in the present application, this procedure appears to have a difficulty in addition to the neglect of the anisotropic motion, which we pointed out made little difference in the  $T_1$  analysis but may make a huge difference in  $T_2$ . This procedure, and the assumptions contained therein, leads to an activation parameter representing the barrier to reorientation of the water molecules at the surface, which on average is equal to or larger than the enthalpy of adsorption or desorption of the water from the protein. That is, the fit gives 11 kcal/mol for the activation barrier while the enthalpy of adsorption is reported to be between 10.5 and 12 kcal/mol for most proteins in the same water content range.<sup>26</sup> Therefore the activation parameter implies a reorientational mechanism in which the water molecules desorb, reorient, and resorb; a process that appears to be energetically unreasonable and inconsistent with

the rapid motions occurring at low temperatures. We conclude that although the distribution of correlation times concept certainly has merit its usual application even when cross relaxation is partly taken into account leads to energetically unreasonable results and also fails to account for the data by itself. Important causes for the discrepancy most likely include (1) the effects of anisotropic rotational motion on  $T_2$  that can depress  $T_2$  relative to  $T_1$  by large factors and (2) the neglect of cross-relaxation contributions to  $T_2$ . We will now examine a third extreme, the absence of any distribution of correlation times and neglect of anisotropic motion.

The  $R_w^{-1}$  data of sample 1H were fitted to the isotropic form of eq 6 by using a nonlinear least-squares program that permitted the two activation parameters and the second moment parameter to vary. The results for these parameters are  $\Delta H = 3.1 \pm 0.1$  kcal/mol,  $\tau_0 = (3.9 \pm 1.2) \times 10^{-12}$  s $^{-1}$ , and  $\sigma_0^2 = (8.9 \pm 0.2) \times 10^9$  s $^{-2}$ . Several features are obvious: (1) The activation barrier obtained in this way is (a) much smaller than when a distribution of correlation times is assumed and much closer to values usually associated with a single hydrogen bond, (b) within 40% of the activation energy obtained from a simple log plot of the transverse-relaxation times  $T_2^*$ , (c) significantly less than that associated with desorption of water from the surface, and (d) more consistent with rapid motion of the water at low temperatures as observed in the present experiments. (2) The second moment is smaller by about a factor of 3 than that appropriate to ice. The last feature is critical and implies that while this simpler approach to the data is remarkably good, there is still something missing in order to account for the major features of the data.

**Combined Model.** It is well known that anisotropic motion may decrease the apparent strength of a magnetic interaction, i.e., decrease the value of the second moment in the above analysis. However, including anisotropic rotation of water as in the model presented earlier leads to small increases, on the order of 50%, in the value of  $T_1$  at the minimum or equivalently in the second moment. Thus, simple anisotropic motion at the H-bond angles assumed earlier falls short of accounting for the inefficiency of relaxation or the elevation of the  $T_1$  minimum. The discrepancy is quantitatively close to a factor of 2. If we examine the elementary anisotropic model proposed earlier, it is clear that the assumption of only two correlation times is undoubtedly oversimplified for several reasons: (1) The water molecule may be hydrogen bonded to the protein in several ways, including H-bond formation through a hydrogen atom of the water molecule or through an oxygen atom of the water molecule. (2) The water molecule may have more than one hydrogen bond to break in order to rotate about the strongest hydrogen bond. (3) The water molecule may make hydrogen bonds to a variety of groups on the protein surface, which are undoubtedly of slightly different strength. Thus, some distribution in activation parameters or correlation times is expected for both the rapid rotation and the slower reorientation of the rotation axis or translation in the anisotropic motion model proposed earlier. A factor of 2 in the elevation of the  $T_1$  minimum for the fast motions may be achieved at the present frequencies by assuming a distribution of correlation times with a  $\beta$  parameter of the order of 3, corresponding to most of the correlation times lying within a factor of 10 of the average value, which seems quite reasonable. A precise evaluation of parameters for a synthesis of anisotropic motions and distributions or correlation times does not appear warranted by the limitations imposed by a finite data set; however, we suggest that such a combination of elementary models is suggested by the data and that such a combination leads to a picture of water molecule motion that is much more reasonable than models that neglect either anisotropic motion or a distribution of correlation times. It is interesting to note that the anisotropic motion model presented earlier inherently provides a distribution in the second-moment parameter. That is, rapid rotation about one axis effectively decreases the value of the apparent second moment. A distribution in  $\Delta$  thus yields a distribution in  $\sigma_0^2$ . To account for the NMR  $^1\text{H}$  relaxation data for the water-lysozyme powder system, we are led to consider both a distribution of second moments, i.e., rotation angles, as well as a distribution of correlation times for the rotations

(25) Belfort, G.; Sinai, N. In "Water in Polymers"; Rowland, S. P., Ed.; American Chemical Society, Washington, D.C., 1980; ACS Symp. Ser. 127, 323-345.

(26) Kuntz, I. D., Jr.; Kauzmann, W. *Adv. Protein Chem.* **1974**, *28*, 239-345.



involved. When both are included, both the magnitudes of the relaxation parameters and the energy barriers fall within physically reasonable limits. The present data do not provide the possibility for assessing the width of a distribution possibly associated with the slow motions in the system, though some distribution is anticipated for all the reasons mentioned above.

**Interpretation of Model Parameters.** The present data leave little doubt that cross relaxation between a rapidly relaxing proton population and a slowly relaxing population dominates the nuclear spin dynamics over much of the temperatures studied. However, restriction of  $R_w$  to describe only intrinsic water relaxation in the absence of the protein surface and protein surface protons in particular is not supported by the data nor by the spirit of the relaxation model. Though an extended discussion of this point is possible, only a few major points are addressed here.

If  $R_w$  characterized only water interactions, we would not find the observed discrepancies between the magnetically deduced and analytical values of  $F$ . More importantly,  $R_w$  would behave differently than reported by Fung and McGaughy<sup>9</sup> as a function of water isotope composition. That is, a large reduction in  $R_w$  is not observed with increasing mole fraction of deuterons in the sample. These authors have argued that  $R_w$  is therefore a parameter that contains inter- as well as intramolecular interactions. Indeed it must. There is no doubt that  $R_w$  contains contributions from water proton-water proton intermolecular interactions since the model contains nothing to exclude such contributions. Further, if we assume a state of high isotope dilution in the water population, the few protons on the adsorbed HOD molecules still move rapidly in the dipolar fields of the nearest neighbor protein protons, and the resulting dipole-dipole contribution to the relaxation will report the rapid water motion. That is, a few protein surface protons are expected to interact strongly with adsorbed water molecules perhaps of somewhat less than 1 proton/water molecule on average and be incorporated as a consequence into the population of rapidly relaxing protons. There may also be small contributions to the rapidly relaxing proton bath from some very rapidly moving longer side chains of the protein. One could argue then in favor of a three-spin bath systems, liquid, solid, and interface. The intimate contact of the liquid with the surface would appear to make the separation unrealistic in the present system, and in addition experimental evaluation of the additional number of parameters implied by such a strategy is unreasonable given the precision and the number of observables. Therefore, while the population characterized by  $R_w$  is clearly dominated by water spins, it is not nor can it be considered to represent a simple intramolecular water proton relaxation rate. This situation places some constraints on the degree of precision that is appropriate or practical in data refinement; however, it should not seriously compromise the primary conclusions of the preceding discussions.

## Conclusion

The present data and analysis provide a basis for understanding

the magnetic properties of water on a protein surface. There is a close coupling of the water proton magnetization with the protein protons through the temperature range from 300 to 130 K, but the direction of flow of magnetization between these two populations is temperature dependent. At low temperatures the water molecule motion is too slow to contribute efficient relaxation sites to the system. Under these conditions the concept of separated spin baths at internal equilibrium is no longer applicable and the effect of the water is to add protons to the relaxation load of the more rapidly rotating methyl groups of the protein. At higher temperatures water rotation provides efficient relaxation paths for the protein protons. The idea of separated spin baths, a slowly relaxing and a rapidly relaxing one, is well supported by detailed analysis of a very substantial data set. However, the strict separation into purely water and purely protein proton baths is an inappropriate approximation since the protons nearest a water molecule on the protein surface include protein protons that also sense the rapid water molecule reorientation.

Analysis of the relaxation parameters derived from the cross relaxation analysis requires inclusion of the effects of anisotropic motion as well as a modest distribution of correlation times for the water motion in order to bring the data analysis into agreement with a physically and energetically reasonable model. The present analysis differs from previous ones in that even approximate inclusion of the effects of anisotropic motion of water still leads to the assumption of a distribution of correlation times, but the required distribution is much narrower and the activation barrier for water molecule motion much smaller than has been required in treatments where the water motion is assumed to be isotropic.

The hypothesis characterizing water motion at the protein surface, which appears to be most consistent with the available data, localizes water molecules to specific protein sites at which local rotation about a hydrogen bond is characterized by narrow-distribution correlation times centered in a range on the order of nanoseconds at room temperatures even in the relatively dry lysozyme powders studied here. By hypothesis, motional averaging of the water orientation is completed by a somewhat slower reorientation of the rapid-rotation axis that provides the possibility of translation of the water on the surface; however, detailed characterization of the slower process is not provided directly by the present data.

**Acknowledgment.** This work was supported by the National Institutes of Health (GM-18719 and GM-25441). We thank Tim Knoblauch for aid with Karl Fischer determinations and computations. Several useful discussions with Professors Bernard Gerstein and Cecil Dybowski concerning rapid recovery receivers is very much appreciated. Several discussions with Dr. Seymour Koenig and Professors Rufus Lumry and Carmel Jolicœur concerning water-protein interactions have been very helpful at different stages of this work and are gratefully acknowledged.

**Registry No.** Lysozyme, 9001-63-2.